Intensity modulation delivery techniques: ''Step & shoot'' MLC auto-sequence versus the use of a modulator

Sha X. Chang,[a] Timothy J. Cullip, and Katharin M. Deschesne
Department of Radiation Oncology, University of North Carolina at Chapel Hill, Chapel Hill, North Carolina 27514

(Received 1 June 1999; accepted for publication 1 March 2000)

Two intensity modulation radiotherapy (IMRT) delivery systems, the ''step & shoot'' multileaf collimator (MLC) auto-sequence and the use of an intensity modulator, are compared with emphasis on the dose optimization quality and the treatment irradiation time. The intensity modulation (IM) was created by a dose gradient optimization algorithm which maximizes the target dose uniformity while maintaining dose to critical structures below a set tolerance defined by the user in terms of either a single dose value or a dose volume histogram curve for each critical structure. Two clinical cases were studied with and without dose optimization: a three-field sinus treatment and a six-field nasopharyngeal treatment. The optimization goal of the latter case included the sparing of several nearby normal structures in addition to the target dose uniformity. In both cases, the target dose uniformity initially improved quickly as the IM level increased to 5, then started to approach saturation when the MLC technique was used. In the absence of the both space and intensity discreteness intrinsic to the MLC technique, the modulator technique produced greater tumor dose uniformity and normal structure sparing. The latter showed no systematic improvement with increasing IM level using the MLC technique. For the sinus tumor treatment of 2 Gy the treatment irradiation time of the modulator technique is no more than that of the conventional treatment. For the MLC technique the irradiation time increased rapidly from 4.4 min to 12.4 min as the IM level increased from 2 to 10. Both clinical cases suggested that an IM level of 5 offered a good compromise between the dose optimization quality and treatment irradiation time. We showed that a realistic photon source model is necessary for dose computation accuracy in the MLC-IM treatments. [S0094-2405(00)03305-8]

Key words: intensity modulation, multileaf collimator, compensator, dose optimization

I. INTRODUCTION

There are several different techniques available for routine clinical treatment delivery of intensity modulation radiation therapy (IMRT) designed by dose optimization algorithms.[1–3] Multileaf collimator (MLC) techniques utilize a built-in or added-on functionality of modern medical accelerators.[4,5] The MLC techniques deliver an intensity modulated photon field by either moving the collimator leaves during irradiation or by irradiating a sequence of static MLC ports. The former is often referred to as the ''dynamic'' MLC technique[2,3,6] and the latter as the ''step & shoot'' MLC auto-sequence technique.[7–10] A less common method of IMRT treatment delivery is the use of a compensatorlike intensity modulator. At the University of North Carolina at Chapel Hill we developed a modulator technique in early 1993 to deliver IMRT, which has been successfully implemented in routine clinical application since 1996.

Compensators of different types have been used over the years to improve dose distributions.[11,12] Initially, they were used to merely compensate for the ''missing tissue'' in the actual patient geometry compared to a rectangular phantom. Although these compensators were developed at a time when 3D image-based treatment planning and dose calculation were not yet available, they are still used today with the aid of skin contour definition tools such as video systems,[13] CT scanners,[14] and Moiré topography.[15] In recent years more sophisticated techniques including the one used in this study were developed whose objectives were no longer to compensate for ''missing'' tissue but for the missing dose.[16–21] We use this technique as an alternative to the MLC techniques to deliver intensity modulated treatments designed by a 3D treatment planning system via a dose optimization algorithm.[22] To mark the distinct difference in objectives between the ''missing tissue'' type compensators and this intensity modulation technique we designate this technique as a modulator IMRT technique. We strongly believe that the objectives of other compensator techniques should no longer be ''skin deep,'' rather, they should adapt to a new role as an alternative IMRT delivery tool.

The major advantage of the ''step & shoot'' MLC delivery technique over the modulator technique is treatment delivery automation. This advantage can become very important when the number of IM treatment fields is large. The advantages of the modulator technique over the ''step & shoot'' MLC technique are much less apparent. A basic difference between the two IM delivery techniques is the resolution of the intensity modulation delivered. The modulator technique generates a continuously varying intensity modulation, as it is created by the dose optimization of clinical cases. Characterized by the finite width of the MLC leaf and

the fact that the treatment is delivered one segment at a time, the ''step & shoot'' MLC-IM technique delivers ''skyscraper''-like intensity modulation maps that are discrete in both intensity level and spatial variation within the IM plane. The actual dose optimization quality delivered is related to how close the delivered IM map is to the intended continuous IM map. This match can be improved by increasing the number of MLC segments used, which is proportional to the intensity resolution as shown in the Results section of this paper.

In the following sections of the paper we evaluate both the ''step & shoot'' MLC technique and the modulator technique for IMRT treatments of two clinical cases. The evaluation is performed in terms of two clinically relevant factors: dose optimization quality specified by the dose optimization goal used and treatment irradiation time. In addition, we present the results of the dependence of the dose optimization quality and the treatment irradiation time on the number of MLC segments. Some other issues important to the study presented will also be discussed.

II. METHODS AND MATERIALS

A. Treatment planning and dose optimization

An in-house 3D treatment planning system, PLanUNC (PLUNC), with a dose gradient optimization algorithm[22] was used for the study. The variables in the dose optimization are restricted to the intensity modulation of the fields and their beam weightings. The number of fields and the geometry of each field including its port must be defined by the user prior to dose optimization. There are different treatment optimization goals used in dose optimization algorithms ranging from dose optimization goals such as dose uniformity of a group of points, within a defined 2D plane, or within a volume; to dose biological effect goals characterized by tumor control and accepted normal tissue complication probabilities,[23,24] as well as hybrids of both dosimetric and dose effect concerns.[25,26] In this study the dose optimization goal was to achieve as uniform a target dose distribution as possible while maintaining the critical structure doses below a set tolerance defined by the user in terms of either dose volume histogram curves or specified maximum dose values for each structure of interest.

The original dose gradient optimization algorithm, used for the first clinical case, is briefly described below. Pencil beams of different intensities are used to assemble the intensity modulation of a field. When the optimization goal is target dose uniformity, the dose gradient (or variation) in the target volume (due to the otherwise open field irradiation) is minimized by adjusting the pencil beam intensities to create the opposite dose gradient thus the net dose gradient is minimized. Only the component of the dose gradient parallel to the IM plane of the field can be minimized by the intensity modulation of the field. The dose gradient component perpendicular to the IM plane can be minimized by varying its beam weighting and/or by modulating the intensity map(s) of other beam(s). Along each pencil beam that passes through the target volume, the point doses were sampled within the target volume. The pencil beam-averaged target dose, defined as the sum of the target point doses along the pencil beam divided by the total number of the points sampled, is calculated. Note that the dose at each sampling point is the total dose contributed from all fields, with and without IM. The same calculation is performed for every pencil beam and for all IM fields, then the relative intensity of each pencil beam is adjusted to attempt to give equal pencil beam-averaged target dose. Because the dose to a point is contributed by almost all pencil beams under the influence of tissue density heterogeneity (a modified BATHO[27] tissue inhomogeneity correction method was used in the dose computation) a full-scale 3D dose computation is performed after each iteration. Several iterations are needed for the optimization process to converge. When the optimization goal includes normal structure dose tolerances the intensity of pencil beams passing through the structures is limited by the tolerance dose set by the user.

Pencil beams used in the calculation had infinitesimal width. Sixty-four pencil beams were sampled uniformly in each IM field. The intensities of the pencil beams between the sampled pencil beams were derived via linear interpolation. The iterative process continues until every pencil beam in the IM fields has the same pencil beam-averaged target dose unless it is limited by the normal structure dose tolerance. When this is achieved, the projection (or the component) of the average dose gradient (over the treatment target) in the IM plane of each IM field is minimized, i.e., the treatment target dose gradient itself is minimized, and the target dose uniformity is thus optimized. The optimization process normally converges within 10 iterations in 30 s of time in our clinical application. The convergence can be conveniently monitored by user on computer display of target volume differential DVH, whose peak height initially grows then cease to grow with further iterations. PLUNC is running on a network of Compaq Professional Workstation XP1000's (True64 Unix) (Compaq, Inc., Houston, Texas) with an X11 window system using Open GL extensions (Silicon Graphics Computer Systems, Inc., Mountain View, California). The Alpha 21264 processor runs at 500 MHz with 512 MBytes of main memory.

Prior to dose optimization the user is required to set the initial condition by assigning conventional beam weighting for each field and by defining which field(s) will be intensity modulated. Treatment fields whose intensities are designated by the user not to be modulated (they still participate in the dose optimization process) can be either open or wedged fields. The beam weightings are the only optimization variables for these fields. The practical benefits of this optimization flexibility will be discussed later in the paper.

Recently we have modified the original dose optimization algorithm and added important versatility in the definition of the optimization goal. The goal can now be defined in terms of either a single dose value or a user-defined dose volume histogram curve for each anatomical structure of interest. An index-dose concept is used to accomplish the new dose optimization utilizing the original dose gradient approach. In brief an index-dose at a point is a product of the physical

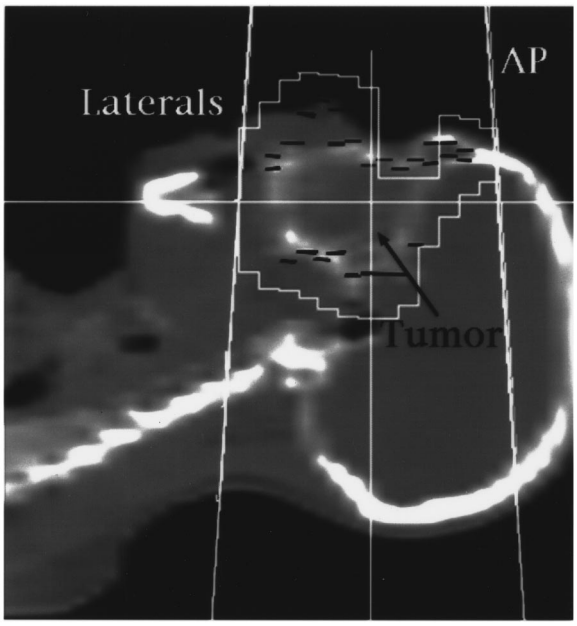

FIG. 1. A sinus tumor treated with a standard three-field setup. The globes were blocked via MLC in all three beams. The same beam setup and ports were used in all IMRT and conventional treatment techniques studied.

dose and a number specific to the location and/or structure association of the point. The index distribution can be manipulated in such a way so the optimization of index-dose gradient throughout the entire treatment volume will generate a dose distribution approaching to the quality specified in the dose optimization goal. This index-dose optimization is used in the second clinical case presented below. Details of this index-dose approach are beyond the scope of this study and will be published separately.

B. Clinical case 1: Sinus tumor

A three-field sinus tumor treatment is shown in Fig. 1. The extensive tumor was primarily located in the ethmoid sinus region between the globes, making tumor dose uniformity and dose sparing to the left globe a treatment planning challenge. The critical structures (globes) were blocked in all three fields. Using the same beam setup, treatment planning was performed using conventional open/wedged fields, dose optimization via modulators, and dose optimization via ''step & shoot'' MLC sequences of different IM resolutions. The original dose gradient optimization algorithm was used for the optimization. The treatment planning goal was the same independent of the treatment technique used: to maximize dose uniformity in the treatment target volume. All three beam ports were defined by MLC regardless of the technique used. This is important for dose volume histogram analysis, where whether the volume is defined by a continuous block or a jagged MLC edge can make a sizable difference. The part of the tumor between the globes was blocked in the two lateral fields, therefore it was considerably underdosed using the conventional wedge technique. All three

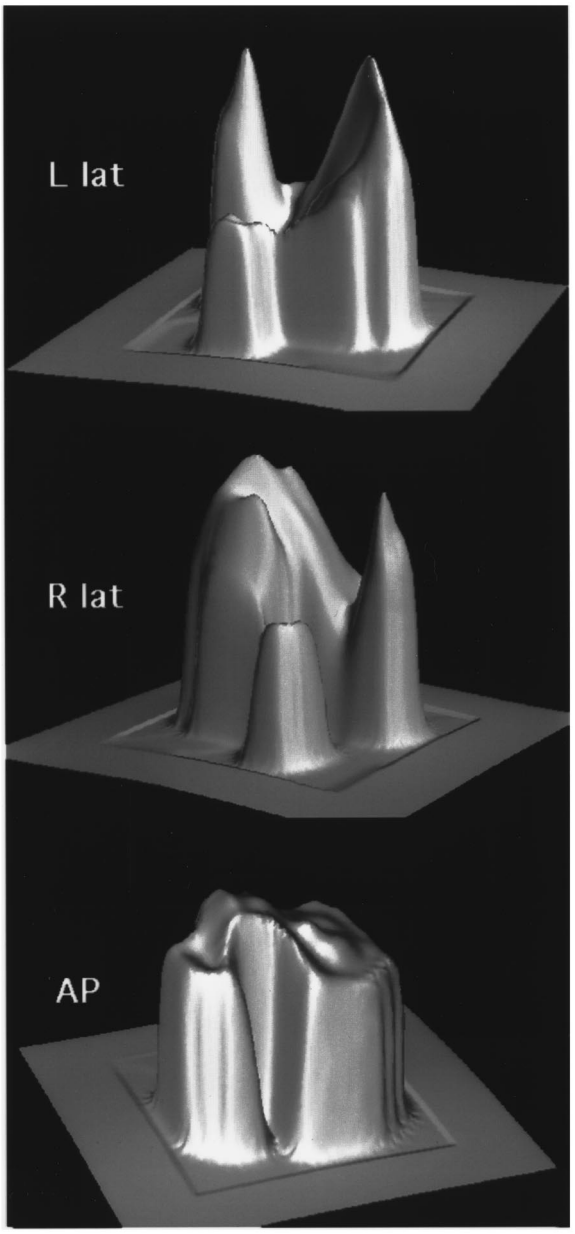

FIG. 2. The intensity modulation (IM) maps of the three-field sinus tumor treatment (Fig. 1) generated by the dose gradient optimization algorithm in PLUNC. The height of the map represents the relative photon fluence intensity within the field.

fields were intensity modulated in the dose optimization. Figure 2 shows the resulting intensity modulation maps for all three fields.

C. Clinical case 2: Six-field nasopharynx tumor treatment

Figure 3 shows the six-field nasopharynx tumor treatment. There are a number of normal structures in the vicinity of the tumor in this case and they require important consideration in addition to the treatment target dose uniformity. The normal structures are cord, globes, chiasm, and the left and right parotid glands. The index-dose gradient optimization algorithm was used for optimization. The dose optimization goal

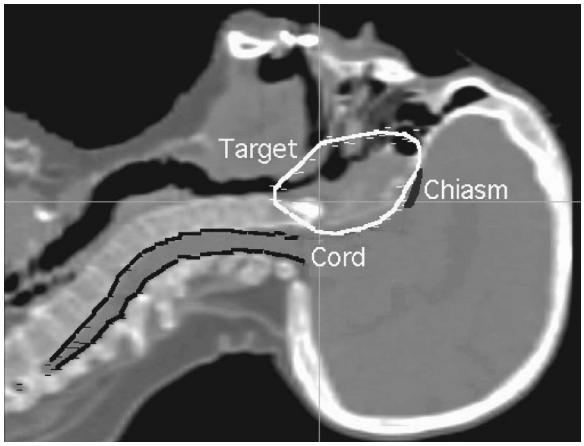

FIG. 3. A nasopharynx tumor treated with a six-field (co-planar) setup. Equal angler separation between adjacent fields was used. The treatment target volume, cord, and chiasm are illustrated. The normal structures of concern not shown in the figure are globes and the left and right parotid glands.

for this case includes the dose uniformity (70 Gy) of the tumor volume and a user-defined dose criterion for each of the normal structures. The cord and the chiasm were limited to a maximum dose of 40 Gy and 30 Gy, respectively. The goal for the globes, left parotid gland, and the right parotid gland were defined in terms of maximum dose volume histograms (DVHs). There is no penalty if the resulting normal structure DVH is better than initially specified. Figure 4 displays an example of the user-defined DVH curve (for globes) as the dose optimization goal. Also displayed in Fig. 4 is the DVH of the initial condition prior to dose optimization. All six fields were intensity-modulated during optimization in the nasopharynx treatment. Two examples of the resulting IM maps are shown in Fig. 5. Compared to the sinus tumor case, where there was less concern of nearby normal tissue sparing, the IM maps in this case had a larger intensity variation with higher spatial frequency. When the maximum range of intensity modulation set in PLUNC is reached one would see the high intensity in the IM map truncated. The maximum IM magnitude setting in PLUNC is 1.8% of the open field intensity. The IM range of the modulator technique is discussed in the section below.

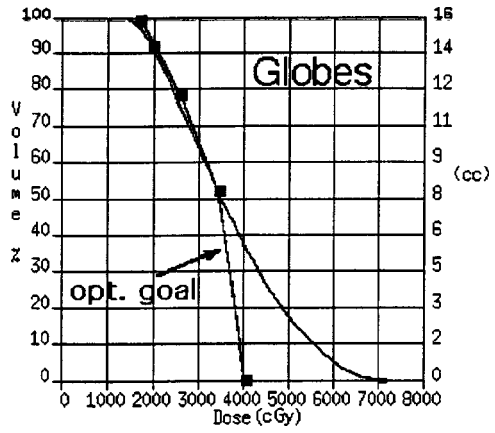

FIG. 4. Dose optimization goal specification in terms of the desired DVH curve (chiasm) for the nasopharynx case. The dots are created by mouse clicking on the DVH curve and used to manipulate the desired DVH shape. The DVH calculated from the initial condition prior to dose optimization is also shown.

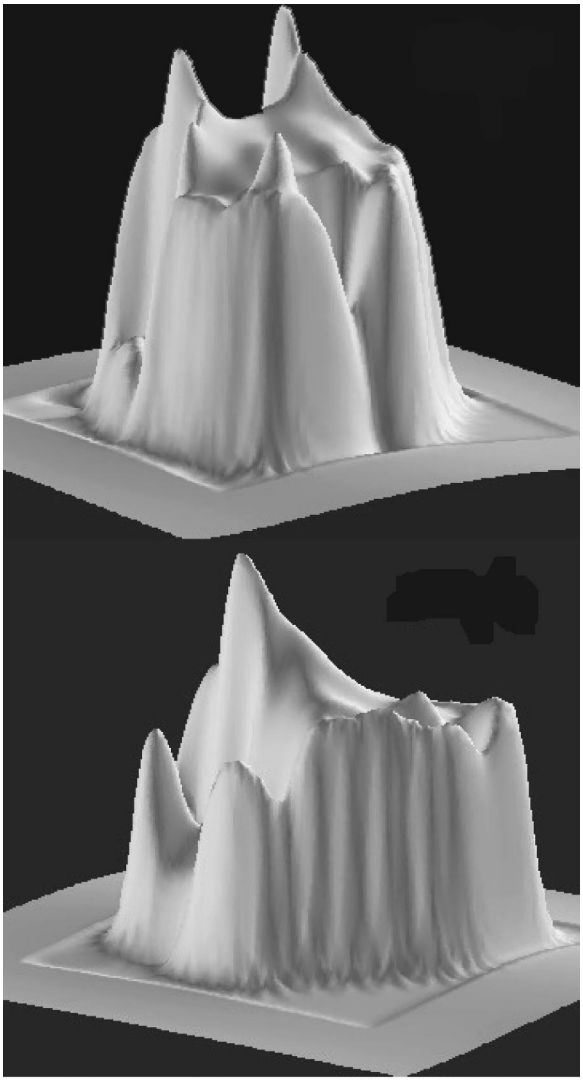

FIG. 5. Two example IM maps of the six-field nasopharynx tumor treatment (Fig. 3), field RPO (upper) and field LAO (lower).

D. Modulator-IM technique

The modulator-IM technique can deliver the IM treatment the way it was originally designed by the dose optimization algorithm. After the dose optimization is completed a modulator file for each IM map is created. The photon fluence attenuation through the modulator is calculated in PLUNC using the exponential equation, $e^{-\mu t}$, where t is the path length of the pencil beam in the modulator. The linear attenuation coefficient μ was determined from the measured data in the following manner. Wedgelike modulators (corresponding to 30°–60° wedges) were made and the beam profiles in the water phantom were measured. We used a path length-dependent μ value to reflect the beam hardening effect, $\mu(t)=\mu_0+ct$. The constants, μ_0 (0.217 for 6 MV;

0.175 for 15 MV) and c (-0.005 for 6 MV; -0.003 for 15 MV), are selected so that the calculated modulator profiles match the corresponding measurement for a variety of the field sizes, depths, and the wedge angles. The increased scatter dose from this medium-density modulator was not observed in percentage depth dose measurements. The study by Chang *et al.*[28] on contralateral breast dose from different tangential breast irradiation techniques including the modulator-IM and the MLC-IM techniques showed that the modulator techniques generated slightly less scatter dose to the contralateral breast than the conventional wedge techniques. The same study also showed that the MLC-IM technique together with the virtual wedge technique produced the least scatter dose to the contralateral breast.

The modulator file [specifically designed for the computer-controlled milling machine (Par Scientific, Model ACD-3, Odense, Denmark)] and the accelerator type (Siemens Medical Systems, Inc., Concord, California) was downloaded from PLUNC to the PC computer that operates the milling machine. The milled styrofoam mold was visually verified for its pattern, dimension, and orientation with respect to the printout of the IM map. A thin plastic sheet was used to cover the opening of the mold with a help of double-sided tape. Through a small filling hole the mold was then tightly packed with small tin granules to a consistent density with the help of an electric massager. The finished tin granule modulator was labeled and placed into a sturdy acrylic box, which can withstand daily clinical handling, and can be easily and correctly inserted into the wedge slot on the accelerator. The styrofoam mold is precisely sized to snugly fit the modulator box, which in turn fits into the wedge slot in the accelerator head as the wedge does. Thus, misalignment of a modulator during treatment is unlikely.

The QA procedure for the modulator-IM treatments includes beam profile and patient *in vivo* dose measurement and comparison. Two IM beam profiles, inplane and crossplane with user-defined offsets, were calculated at the measurement condition and compared to the measurement for each modulator prior to the first treatment. The Profiler detector system (SunNuclear Corporation, Melbourne, Florida), a PC computer-controlled beam profile measurement system equipped with a linear array of diode detectors separated by 5 mm, was used for the measurement and its real time comparison to the calculation. The calculated beam profiles were downloaded to the Profiler computer prior to the measurement. Using the ''overlay'' display feature, the comparison between the calculated and measured beam profile is accomplished in real time during the irradiation. We find this real time comparison to be a very valuable feature for routine clinical modulator application where timely and informative QA procedures are much needed.

A patient skin dose measurement using MOSFET detectors (Thomson & Nielsen Electronics Ltd., Ontario, Canada) is also performed and compared to the dose calculated by PLUNC within the first 10 Gy of dose delivery. The measured dose is compared with the calculated dose at the measurement location. The IMRT modulator QA procedures[29] were carefully followed in each step of the fabrication and dosimetric verification processes for all clinical modulators. A summary of the QA results of the clinical IMRT modulators for the past several years, together with the dose optimization results, is currently being prepared for publication. The lowest photon intensity achieved by the current tin granule type of modulator is 38.3% and 44.9% of the open field for 6 MV and 15 MV beam, respectively. However, this range can be easily increased by replacing the tin granules with a material of higher effective density and/or by increasing the maximum thickness of the modulator (currently 5 cm) without further modification of the technique.

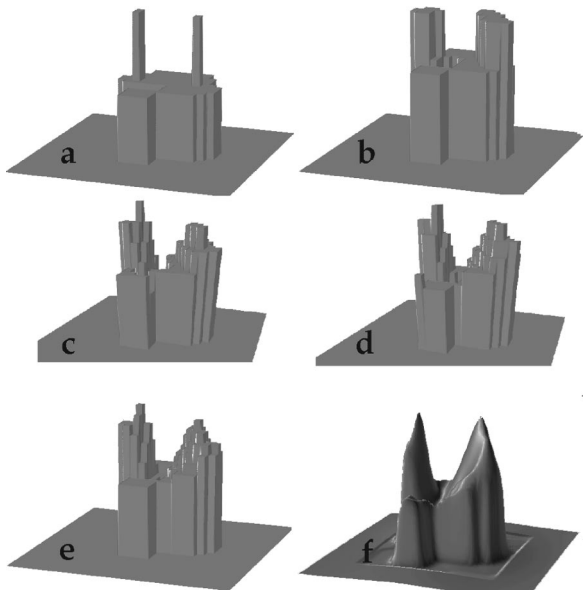

FIG. 6. Discrete IM maps [(a)–(e)] converted from the smooth IM map (f) originally generated by the dose optimization algorithm for the left lateral field of the three-field sinus treatment. The intensity modulation resolution of each map is represented by an IM level, which is the number of intensity levels (after common background subtraction) used to construct the IM map. The IM levels used in the maps were (a) 2, (b) 3, (c) 5, (d) 7, and (e) 10 as shown.

E. ''Step & shoot'' MLC technique

To deliver the IM fields via the MLC technique, each of the original IM maps (Figs. 2 and 5) generated by the dose optimization was converted into the corresponding ''skyscraper''-like discrete map. The discrete IM map is created from the original map using a user defined level of discreteness, i.e., IM level. If an IM level of 5 is used, the original map is divided into 5 levels of intensity after the common background subtraction. Figure 6 shows a set of discrete IM maps converted from the original IM map of the left lateral field in the sinus tumor case. Each of the discrete IM maps has a different intensity resolution represented by the number of IM levels used in constructing the IM map. Once the dose optimization was performed and the ''step & shoot'' MLC technique was chosen, PLUNC converted the original IM maps to their corresponding discrete maps with a user-defined number of IM levels.

The discrete IM maps were then input to a stand-alone MLC sequence optimization software system IMFAST (Si-

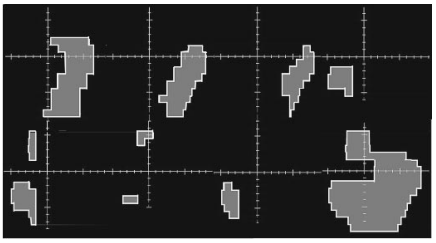

FIG. 7. The MLC segments (8) of the left lateral field of the sinus treatment for the ''step & shoot'' MLC-IM treatment where 5 IM levels were used. The segment with the largest area, or the base segment, shows the treatment portal.

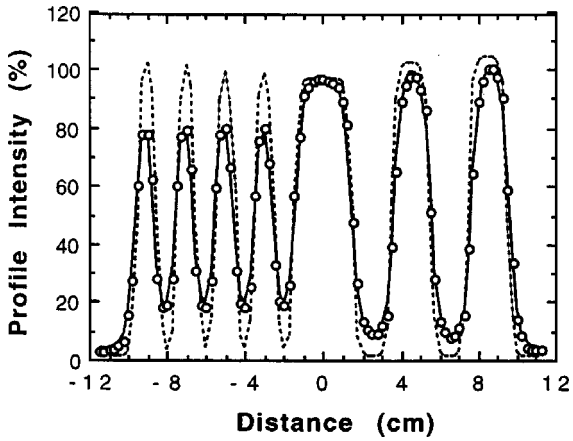

FIG. 8. Comparison of calculated beam profiles by two different photon source models (used in the treatment planning system) and the measurement on a test MLC pattern. The realistic photon source model, composed of a dual Gaussian-distribution source, produced a calculated dose profile (solid line) very similar to the measurement (circles). The calculated dose from a source model having a single small Gaussian distribution only (dashed line) generated a considerable discrepancy with the measurement under this test MLC configuration.

emens Medical Systems, Inc., Concord, California), which generated an optimal sequence of MLC segments and the corresponding monitor units (MU) for a given fractional treatment dose. IMFAST takes into account the mechanical constraints of the MLC leaf positioning, the ''tongue & groove'' effect,[30] a simple photon source model fitted to the accelerator beam data, and other relevant parameters in the MLC sequence optimization. There are several different sequence optimization methods available in IMFAST all of which minimize the number of MLC segments, the treatment delivery time, and to deliver the IM field as close to the input discrete IM map as possible. Siochi[31] has reported the details of the MLC sequencing optimization method used for this study. Figure 7 shows the MLC sequence generated by IMFAST for the left lateral field of the sinus tumor case using a 5 IM level discrete IM map. The MLC-IM treatment is delivered on a Siemens digital Mevatron accelerator retrofit with MLC using Primeview (Siemens Medical Systems, Inc., Concord, California), a treatment delivery automation, record, and verify system when used together with Lantis Record & Verify system (Siemens Medical Systems, Inc., Concord, California). All segments of the same IM field can be grouped together and delivered automatically with a keyboard operation similar to the delivery of a single field.

Using the same MLC segment optimization method, PLUNC independently generated a set of MLC segments which were identical to the one by IMFAST but which had a slight difference in monitor units for segments which were very narrow in one dimension. This is primarily due to the difference in photon source distribution modeling between PLUNC and IMFAST. PLUNC uses a two-source model[32] in which each source has a Gaussian intensity distribution, whereas IMFAST assumes the source intensity distribution is exponential. Realistic photon source modeling plays an important role in the accuracy of dose/MU computation when a portion of the field is very narrow, a situation uncommonly seen in conventional treatment fields but frequently encountered in the ''step & shoot'' MLC technique. We adjusted the parameters in the two-source model (relative strength, relative location, and the size of each source) until the calculated dose distribution was in good agreement with measurement under several irregular MLC segment configurations. Figure 8 shows a beam profile comparison between measurement and calculation for a test MLC field composed of 1 cm gaps on one side of the central axis and 2 cm gaps on the other with a 3 cm gap centered on the central axis. A 6 MV photon field of 40 cm length and a Profiler diode array detector system were used for data measurement (d_{max} perpendicular to the MLC leaf travel direction). Figure 8 clearly illustrates the importance of utilizing realistic photon source modeling in the MLC segment dose/monitor unit calculation.

III. RESULTS

Treatment plans were made for each clinical case with and without dose optimization via intensity modulation. IMRT delivery techniques used here are ''step & shoot'' MLC-IM and modulator-IM.

A. IM resolution versus MLC segments

We found that for the MLC-IM treatment technique there is a linear proportionality between the number of IM levels used and the number of MLC segments required as calculated by IMFAST as shown in Fig. 9. The proportionality is between 1 to 2 segments per IM level per field for both the three-field sinus tumor treatment (left *Y*-axis) with relatively simple IM patterns and the six-field nasopharynx tumor treatment (right *Y*-axis) with more complex IM patterns. The relationship of IM resolution, dose optimization quality, and treatment irradiation time are presented in the following sections.

B. Dose optimization quality

The dose optimization quality of each treatment technique was judged by how well the defined optimization goal was reached for each case.

1. Sinus tumor case

The dose optimization goal for the sinus tumor treatment was dose uniformity in the target volume. The quality of

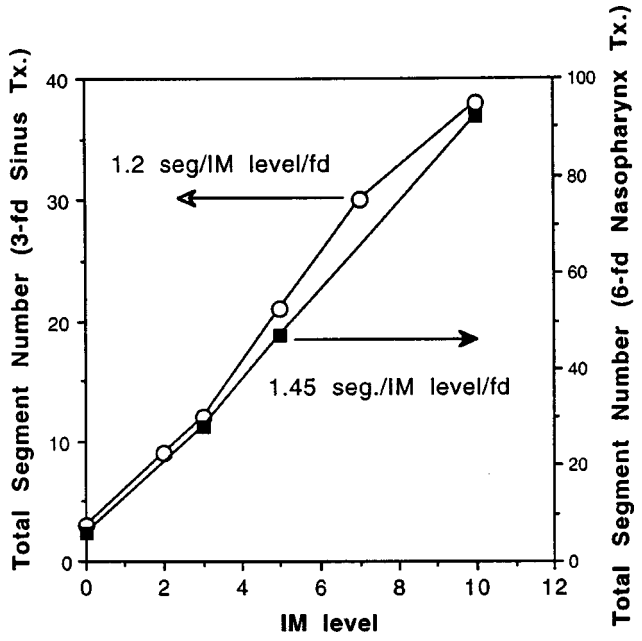

FIG. 9. The total number of MLC segments required vs the IM level used in the ''step & shoot'' MLC-IM treatment technique for the three-field sinus (left *Y*-axis) and the six-field nasopharynx (right *Y*-axis) treatment. The data show that 1.2 and 1.45 MLC segments per field are required for each IM level used for the treatments, respectively.

critical structure (globe) sparing was not considered in the comparison because (1) globes were outside the treatment ports and (2) each treatment port was defined by the same MLC leaf configurations for all techniques. For this case we defined the dose optimization quality as Uniform Dose Volume (UDV) alone. Derived from the differential dose volume histogram of the target volume, shown on Fig. 10(a) for the nasopharynx case, UDV is the percentage of the treatment target volume that receives within $\pm 5\%$ of the nominal dose. The dependence of UDV on the intensity resolution of the IM map is displayed in Fig. 10(b) (left *Y*-axis). The solid horizontal line in Fig. 10(b) represents the UDV value of the modulator technique. The data show that for the three-field sinus treatment at least 3 IM levels were required for the MLC-IM treatment to achieve better dose uniformity compared to the conventional treatment technique (UDV $=75\%$). The UDV quickly improved with increasing IM level initially then approached saturation at an IM level of 5. The UDV only improved from 82% to 83% as the IM level changed from 5 to 10. The gap between the UDV values of the modulator-IM (87%) and the 10 IM level MLC-IM (83%) is one-third of the total difference between the conventional treatment (75.5%) and the optimized treatment with no limit in IM resolution (87%).

2. Nasopharynx tumor case

The dose optimization quality of this nasopharynx tumor treatment is judged by how well all the prerequisites specified in the dose optimization goal have been reached. They include target volume dose uniformity and a set of specified DVH curves or single dose values for the nearby normal structures of interest in addition to tumor dose uniformity.

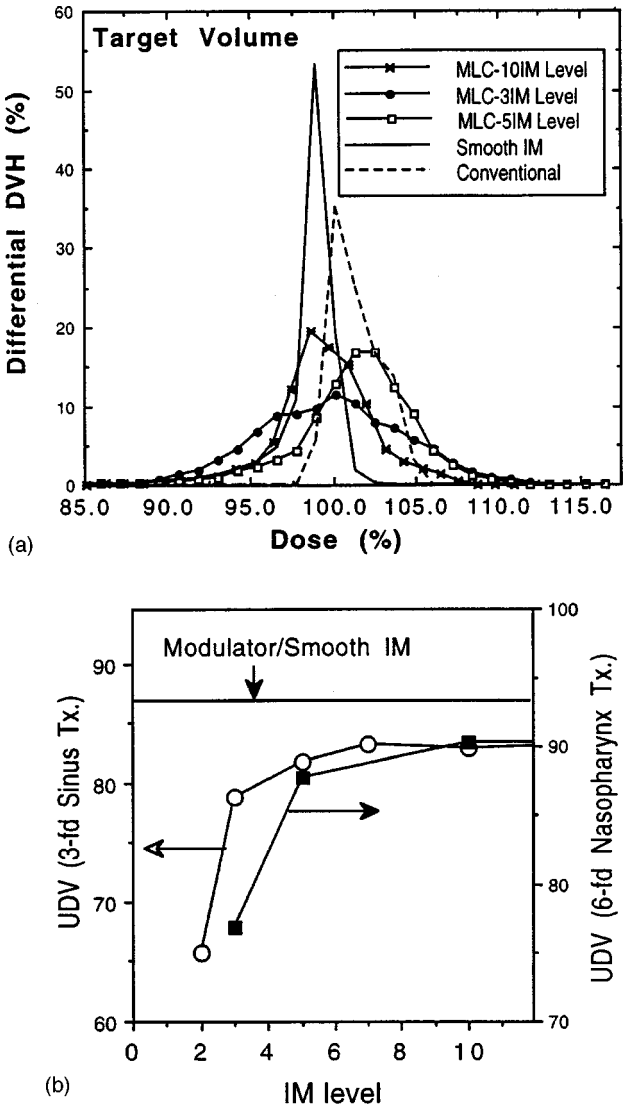

FIG. 10. (a) Differential DVH of nasopharynx target volume; the peak height is related to UDV value. (b) Uniform Dose Volume (UDV) as a function of IM level for the three-field sinus tumor (left *Y*-axis) and the six-field nasopharynx tumor (right *Y*-axis) treatment. UDV represents tumor dose uniformity and is defined as the percentage of the tumor volume receiving $\pm 5\%$ of the nominal dose. The same solid horizontal line in Fig. 10(b) represents the UDV values of the modulator/smooth IM technique for both clinical cases. The smooth IM can be achieved using a modulator similar to the one discussed in this paper. The treatment ports defined by MLC are identical for all IM delivery techniques.

Figure 10(b) (right *Y*-axis) shows one aspect of this multifactored dose optimization quality, the UDV, as a function of IM level for the MLC technique together with the data from the modulator-IM technique. One sees a similar trend in the dependence of UDV on the IM levels for both clinical cases presented: improvement in UDV slows down after the IM level reaches 5. The gap in UDV value between the modulator-IM technique (93.1%) and the 10 IM levelMLC-IM technique (90.4%) is smaller than that of the sinus tumor case. We want to clarify that the IM magnitudes of some of the fields in this case exceed the limit of the current tin granule modulator. The label ''modulator-IM'' in Figs. 10 and 11 is replaced by ''smooth IM'' to reflect this

fact. As we mentioned earlier, this IM limitation can be significantly improved by using a higher effective density modulator material than tin granules.

Manual treatment planning using the conventional treatment technique (wedges and open fields) was extremely difficult and planner-dependent in this six-field case with a complex dose optimization goal. It was relatively easy to manually achieve tumor dose uniformity but not while simultaneously sparing the normal structures as specified in the dose optimization goal. For this reason this planner dependence of the conventional treatment plan should be noted if the plan is used for a reference of comparison.

In terms of the other aspect of the dose optimization quality, the normal structure sparing, the evaluation method used is much less systematic and quantitative but informative. Figure 11 shows the degradation in the dose sparing of the MLC-IM technique with different IM resolutions for some of the normal structures (cord, chiasm, and left parotid) in terms of DVH. Similar results are also seen in DVHs of other normal structures not shown here. The data from the corresponding conventional and the modulator-IM techniques are also displayed in Fig. 11. It is interesting to see that the differences in DVHs between the modulator-IM technique and the MLC-IM techniques are not closely related to the IM level used. This phenomenon strongly suggests that the spatial resolution of the MLC-IM technique (1 cm×1 cm), which is unchanged as the IM level increases, is responsible for the difference in the nearby normal structure sparing between the modulator-IM and the MLC-IM techniques.

C. Treatment irradiation time

The treatment irradiation time is defined as the time elapsed between the initiation of the treatment on the accelerator console by pushing the ''rad on'' button to the completion of the irradiation. Besides the treatment irradiation time defined above, the conventional and the modulator-IM techniques require additional time for therapists to enter the treatment room to exchange the modulator or wedge between treatment fields. This beam modifier exchange time is generally no more than 45 s in our clinic. We defined *equivalent treatment irradiation time* as the treatment irradiation time plus the beam modifier exchange time when applicable for a meaningful inter-comparison of treatment irradiation time among the MLC-IM technique, the modulator-IM technique, and the conventional technique. The treatment irradiation times were measured using a stopwatch for a treatment dose of 2 Gy. Figure 12 displays the dependence of the *equivalent treatment irradiation time* on the IM resolution or the IM level for the three-field sinus tumor treatment. The modulator-IM and the conventional wedge technique were included on the graph for comparison. Figure 12 reveals that the *equivalent treatment irradiation time* increased quickly from 5.6 to 13.8 min as IM levels increased from 2 to 10. The modulator-IM and the conventional treatment techniques required substantially less treatment irradiation time (3.2 min).

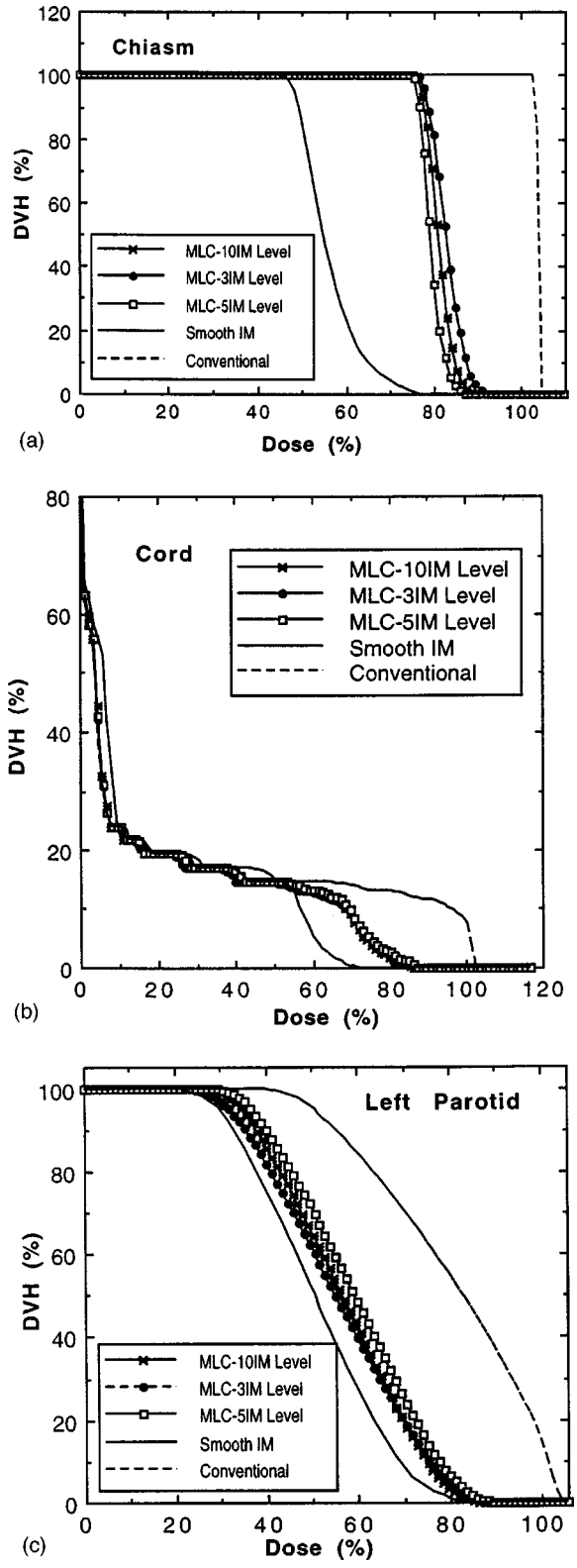

FIG. 11. DVHs of the normal structures from conventional and different IM delivery techniques for the nasopharynx case: (a) chiasm, (b) cord, and (c) left parotid gland.

D. Comparison of the IM delivery techniques

The inter-dependence between the dose optimization quality and the treatment irradiation time for the MLC-IM

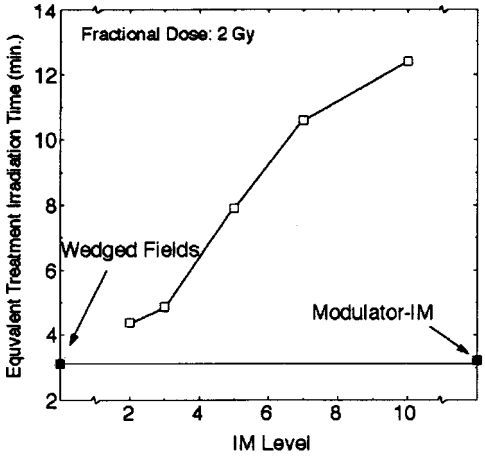

FIG. 12. The Equivalent Treatment Irradiation Time as a function of the IM level for the three-field sinus tumor treatment. In addition to the irradiation time itself, the equivalent treatment irradiation time includes the extra time required (45 s per exchange) for a therapist to enter the treatment room and to manually exchange the wedge/modulator between treatments of different fields when applicable. The data of the conventional wedge technique and the modulator-IM technique were also included in the graph for the sake of comparison.

technique in the sinus tumor treatment is shown jointly by Figs. 10(b) and 12. The former required more IM levels for better dose optimization quality which in turn demanded more treatment irradiation time. The dose optimization quality represented by UDV approached saturation at an IM level of 5 whereas the treatment irradiation time increased briskly with increasing IM levels. An IM level of 5 seemed to be a good compromise between the dose optimization quality and the treatment irradiation time for the MLC-IM technique. Even though the optimization goal included both normal structure sparing and treatment volume dose uniformity for the nasopharynx tumor case, the IM level effect of the MLC-IM technique manifested itself primarily in the target dose uniformity, as evidenced by Figs. 10 and 11.

We have demonstrated that the modulator technique established the upper limit for the quality of dose optimization, whereas the conventional technique via open and wedged beams established the baseline for the treatment irradiation time. It is apparent from Fig. 12 (three-field sinus treatment) that the modulator technique required no additional time in treatment delivery compared to the conventional technique while the MLC-IM techniques required considerably longer time (100%–400%) to deliver the treatment. The total patient treatment time, which includes but is not limited to the irradiation time described thus far, will be discussed later.

E. IMFAST verification

An ''error map'' is defined in IMFAST as the difference between the input (skyscraper) intensity map and the IMFAST-produced ''step & shoot'' MLC-IM intensity map. This ''error map'' is a quick yet informative presentation of the quality of the MLC segment sequence optimization to users. We independently verified an ''error map'' along the inplane direction on the central axis for the left lateral sinus field. The measured ''error map'' is the difference between the discrete intensity map calculated by PLUNC and the measurement from the MLC-IM field delivery. The average deviation between the predicted (by IMFAST) and measured ''error map'' in the measurement region was less than 2%; results in other regions of the IM map were similar.

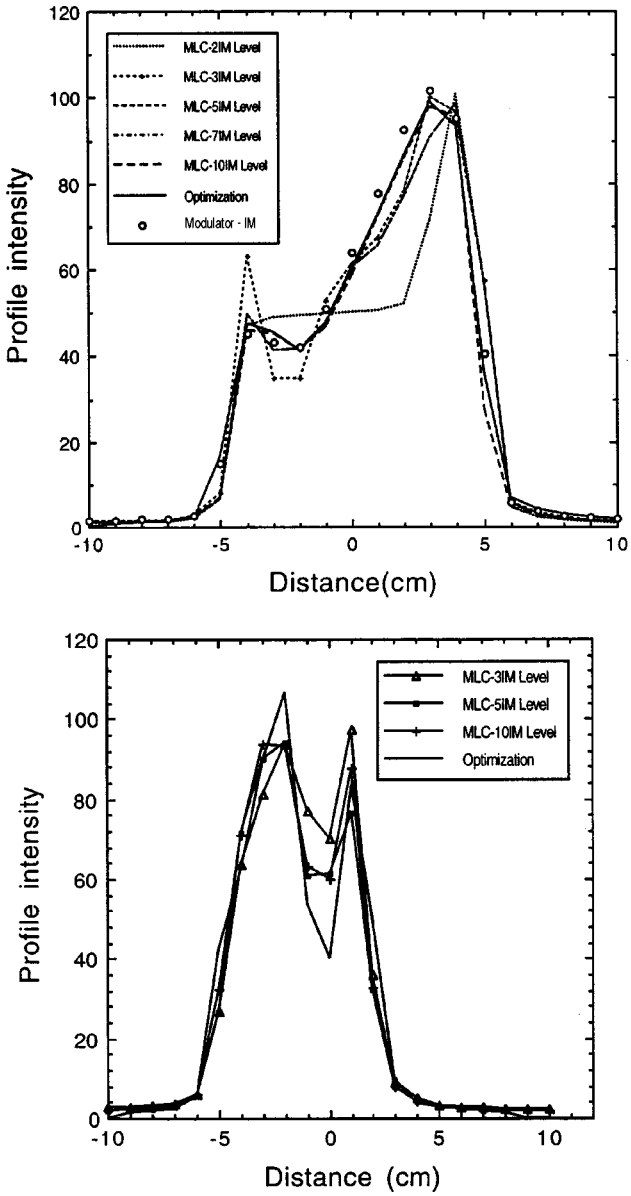

FIG. 13. Profile comparison of the original IM map generated by the dose optimization algorithm and the actual measured IM maps delivered by different IM treatment delivery techniques (modulator technique and ''step & shoot'' MLC-IM techniques of different IM level). (a) Right lateral field of the sinus treatment case, and (b) RAO field of the nasopharynx treatment case.

F. IM quality evaluation

Figure 13 shows the profile comparison between the original IM map generated by the dose optimization algorithm and the actual IM maps delivered by the modulator and the MLC techniques for the sinus case (a) and the nasopharynx case (b). The Profiler array detector system was used for

measurement and comparison. The measurement setup was 80 cm SSD, depths of 2 cm and 4 cm for 6 MV and 15 MV photon beams, respectively. The quality of IM of each technique reflected in the beam profile comparison appears to be consistent with the dose optimization quality shown in Figs. 10–11 previously.

IV. DISCUSSION

A. Fractional monitor unit (MU)

If the total number of segments per MLC-IM treatment is large due to either a large number of IM fields and/or a large number of IM levels, many segments might deliver only very small MUs. When the accelerator cannot deliver fractional MUs the dose round-off error in this case could be sizable. For the sinus tumor case, the minimum segment MU was 2 for the 10 IM level MLC-IM treatment of 2 Gy per fraction. In this case the round-off error for these segments was as high as 25%. The cumulative round-off error over the entire treatment, however, was significantly smaller, and this is supported by the study of IM profile of different IM levels shown in Fig. 12. However, eliminating those MLC segments which have only a few MUs has become an acceptable and common practice in ''step & shoot'' MLC-IMRT. One should realize that doing so further deteriorates the resolution of the IM delivered and therefore widens the difference between the original IM and the actual IM delivered. This fractional MU issue is irrelevant to the calculated results presented in this paper because PLUNC considers fractional MU in its dose computation. The MU truncation is performed when the treatment setup data are downloaded from PLUNC to Lantis treatment record and verify system.

B. The UDV saturation behavior

The UDV saturation behavior seen in Fig. 10(b) can be interpreted as the upper limit of the IM level effect on the target dose uniformity for the MLC-IM technique. An IM treatment delivered by the modulator technique can be viewed as a high resolution MLC-IM treatment with hundreds of IM levels and hundreds of MLC leaves. The gap between the saturation UDV value of the MLC-IM technique and that of the modulator-IM technique is related to the finite spatial resolution (1 cm) of the MLC technique, which is kept the same for all IM levels used. The UDV saturation behavior of the MLC technique is suspected to be related to the closeness of the collimator angle used to the optimal collimator angle. The collimator angle, or the orientation of the MLC leaves, can have significant influence on the discrepancy between the discrete ''sky-scraper'' IM map created for (and delivered by) the MLC technique and its corresponding original smooth map. The effect of the collimator angle is similar to that in conforming a MLC opening to a given treatment portal defined by a block. An optimal collimator angle can minimize the field edge jaggedness; an optimal collimator angle can also reduce the difference between the discrete IM map and its original smooth map. The orientation of MLC leaves (the collimator angle) should be considered as a variable in the MLC-IM treatment delivery optimization process. We are currently in the process of incorporating such a concept into PLUNC for the MLC-IM treatment delivery technique.

C. Treatment automation and treatment time

Gantry and couch movements of newer digital accelerators, which are often equipped with MLC functionality, can also be controlled remotely from the accelerator console. These functions, coupled with Primeview or other advanced treatment automation and record and verify systems, can result in substantial timesaving in total patient treatment delivery. However, this was not included in our treatment irradiation time analysis because these timesavings are not unique to the ''step & shoot'' MLC-IM technique—they apply to all treatment techniques studied which were delivered from the same accelerator. The combined potential timesaving due to the newer generation of digital accelerators and record and verify systems plus the ''step & shoot'' MLC-IM technique itself is highly clinically relevant and deserves separate study.

D. Time required other than treatment delivery

Although we intended to focus on the dose optimization quality and the treatment irradiation time in this study, the comparison between the two IMRT delivery techniques would be incomplete without mentioning the efforts required outside treatment irradiation. This includes the work and time involved in IM treatment preparation and QA procedures. In our clinic it normally takes a trained medical physics technician, who is also responsible for block fabrication, an average of 20 min to complete one modulator. This also includes the time to perform the appropriate QA checks during the fabrication process. Obviously, the MLC-IM techniques eliminate this time consuming IM preparation process. However, once the modulator is made, there is virtually no difference between IMRT via modulator and a conventional treatment in terms of treatment delivery, record keeping, QA via port film and chart check procedures. As described earlier, the dosimetric QA procedure for the modulator-IM technique includes (1) the IM profile measurement and its comparison to the calculation and (2) *in vivo* patient dose measurement and its comparison to calculation. The amount of time for clinical physicists to conduct these QA procedures is on average 30 min per case.

E. Optimization with open and wedged beams

Independent of the treatment delivery technique chosen, the workload required to accomplish an IMRT treatment can be significant. The workload is directly proportional to the number of intensity modulated fields used. For this reason we have purposely been minimizing the number of intensity-modulated fields in the dose optimization. Because the dose optimization algorithm is based on dose gradient rather than dose itself there are a number of approaches possible to minimize the existing dose gradient. It gives the user the flexibil-

ity to designate each beam in the plan to be either open, wedged, or intensity-modulated. All beams participate in the dose optimization process, i.e., the dose optimization is based on the dose distribution from all beams. The dose gradient optimization algorithm finds the most appropriate beam weightings and/or the intensity modulation map for each beam. In many clinical situations, we found that reducing the number of intensity-modulated fields considerably reduced the workload involved for both types of IMRT delivery techniques. The reduction was done only when there would be minimal compromise on the quality of dose optimization. When the IM magnitude required is very large and outside the limit of the modulator technique we often use a combination of wedged and IM fields in the dose optimization as long as the desired IM has a uniform slope component which can be created by the wedged field.

V. CONCLUSION

We have presented comparisons between the ''step & shoot'' MLC auto-sequence and the modulator techniques for intensity modulated treatments created by a dose gradient optimization algorithm for two clinical cases. We have shown that for the MLC-IM technique the treatment irradiation time increased swiftly as the IM resolution improves. However, target volume dose uniformity initially improves with the increasing IM resolution then approaches saturation below the value achieved by the modulator technique. The quality of normal structure sparing in the nasopharynx case is less than that of the modulator technique; there was no close correlation to the IM resolution of the MLC-IM technique. We found an IM level of five to be a good compromise between irradiation time and dosimetric quality for both cases. The more favorable results of the modulator-IM technique can be attributed to its high IM resolution. The use of a modulator can deliver IMRT as it was originally designed without degradation.

Finally, we would like to point out that the main objective of this paper was to evaluate the two IMRT treatment delivery techniques. Although only two related dose optimization algorithms and one MLC segmentation method were used in this study we believe the conclusions are likely to hold, at least qualitatively, for other MLC segmentation methods and dose optimization algorithms which generate continuous IM maps.

ACKNOWLEDGMENTS

The authors are grateful to Drs. Edward L. Chaney and Joel E. Tepper for the helpful discussion and the constructive comments during the preparation of the original manuscript, and Larry Potter for his valuable comments on the revised version. The authors would also like to acknowledge Dr. Alfredo Siochi of Siemens Medical Systems for providing assistance with the IMFAST application, and Elizabeth P. Miller for her contribution to the early development of the modulator IMRT technique, and, finally Dr. Julian Rosenman for his suggestion of the modulator material and for pursuing modulator-IM clinical application.

[a]Address correspondence to: Sha X. Chang, Department of Radiation Oncology, University of North Carolina at Chapel Hill, Chapel Hill, NC 27514, Phone: (919)966-1101, Fax: (919)966-7681, Electronic mail: chang@radonc.unc.edu

[1] A. Wu, M. Johnson, A. S. Chen, and S. Kalnicki, ''Evaluation of dose calculation algorithm of the Peacock system for multileaf intensity modulation collimator,'' Int. J. Radiat. Oncol., Biol., Phys. **36**, 1225–1231 (1996).

[2] L. Ma, A. L. Boyer, L. Xing, and C. M. Ma, ''An optimized leaf-setting algorithm for beam intensity modulation using dynamic multileaf collimators,'' Phys. Med. Biol. **43**, 1629–1643 (1998).

[3] S. Soderstrom and A. Brahme, ''Which is the most suitable number of photon beam portals in coplanar radiation therapy?'' Int. J. Radiat. Oncol., Biol., Phys. **33**, 151–159 (1995).

[4] P. Xia, P. Geis, L. Xing, C. Ma, D. Findley, K. Forster, and A. Boyer, ''Physical characteristics of a miniature multileaf collimator,'' Med. Phys. **26**, 65–70 (1999).

[5] I. J. Das, G. E. Desobry, S. W. McNeeley, E. C. Cheng, and T. E. Schultheiss, ''Beam characteristics of a retrofitted double-focused multileaf collimator,'' Med. Phys. **25**, 1676–1684 (1998).

[6] T. LoSasso, C. S. Chui, and C. C. Ling, ''Physical and dosimetric aspects of a multileaf collimation system used in the dynamic mode for implementing intensity modulated radiotherapy,'' Med. Phys. **25**, 1919–1927 (1998).

[7] A. Eisbruch, L. H. Marsh, M. K. Martel, J. A. Ship, R. Ten Haken, A. T. Pu, B. A. Fraass, and A. S. Lichter, ''Comprehensive irradiation of head and neck cancer using conformal multisegmental fields: assessment of target coverage and noninvolved tissue sparing,'' Int. J. Radiat. Oncol., Biol., Phys. **41**, 559–568 (1998).

[8] J. M. Galvin, X. G. Chen, and R. M. Smith, ''Combining multileaf fields to modulate fluence distributions,'' Int. J. Radiat. Oncol., Biol., Phys. **27**, 697–705 (1993).

[9] S. Webb, ''Configuration options for intensity-modulated radiation therapy using multiple static fields shaped by a multileaf collimator. II: Constraints and limitations on 2D modulation,'' Phys. Med. Biol. **43**, 1481–1495 (1998).

[10] P. Xia and L. J. Verhey, ''Multileaf collimator leaf sequencing algorithm for intensity modulated beams with multiple static segments,'' Med. Phys. **25**, 1424–1434 (1998).

[11] W. Ansbacher, D. M. Robinson, and J. W. Scrimger, ''Missing tissue modulators: Evaluation and optimization of a commercial system,'' Med. Phys. **19**, 1267–1272 (1992).

[12] D. M. Robinson and J. W. Scrimger, ''Optimized tissue modulators,'' Med. Phys. **17**, 391–396 (1990).

[13] J. W. Andrew, J. E. Aldrich, M. E. Hale, and J. A. Berry, ''A video-based patient contour acquisition system for the design of radiotherapy modulators,'' Med. Phys. **16**, 425–430 (1989).

[14] P. A. Jursinic, M. B. Podgorsak, and B. R. Paliwal, ''Implementation of a three-dimensional compensation system based on computed tomography generated surface contours and tissue inhomogeneities,'' Med. Phys. **21**, 357–365 (1994).

[15] A. L. Boyer and M. Goitein, ''Simulator mounted Moiré topography camera for constructing compensating filters,'' Med. Phys. **7**, 19–26 (1980).

[16] S. B. Jiang and K. M. Ayyangar, ''On modulator design for photon beam intensity-modulated conformal therapy,'' Med. Phys. **25**, 668–675 (1998).

[17] L. Brown, A. T. Redpath, and I. H. Kunkler, ''The use of modulators to improve dose homogeneity in breast irradiation with tangential fields,'' in *Proceedings of the XIIth ICCR*, edited by D. D. Leavitt and G. Starkschall, Salt Lake City, UT (Medical Physics, Madison, WI, 1997), p. 483.

[18] J. Stein, K. Hartwig, S. Levegrun, G. Zhang, K. Preiser, B. Rhein, J. Debus, and T. Bortfeld, ''Intensity-modulated treatments: Modulators-vs-multileaf modulation,'' in *Proceedings of the XIIth ICCR*, edited by D. D. Leavitt and G. Starkschall, Salt Lake City, UT (Medical Physics, Madison, WI, 1997), pp. 338–341.

[19] O. C. L. Haas, J. A. Mills, K. J. Burnham, D. E. Bonnett, and A. R. Farajollahi, ''Achieving conformal dose distribution via patient specific modulators,'' in *Proceedings of the XIIth ICCR*, edited by D. D. Leavitt and G. Starkschall, Salt Lake City, UT (Medical Physics, Madison, WI, 1997), p. 483.

[20] G. S. Mageras, R. Mohan, C. Burman, G. D. Barest, and G. J. Kutcher, ''Modulators for three-dimensional treatment planning,'' Med. Phys. **18**, 133–140 (1991).
[21] P. M. Evans, E. M. Donovan, N. Fenton, V. N. Hansen, I. Moore, M. Partridge, S. Reise, B. Suter, J. R. N. Symonds-Tayler, and J. R. Yarnold, ''Clinical implementation of compensators in breast radiotherapy,'' Radiother. Oncol. **49**, 255–265 (1998).
[22] S. X. Chang, T. Cullip, E. P. Miller, and J. Rosenman, ''Dose gradient optimization,'' Med. Phys. **23**, 1072 (1996).
[23] M. Asell, S. Hyodynmaa, S. Soderstrom, and A. Brahme, ''Optimal electron and combined electron and photon therapy in the phase space of complication-free cure,'' Phys. Med. Biol. **44**, 235–252 (1999).
[24] M. Alber and F. Nusslin, ''An objective function for radiation treatment optimization based on local biological measures,'' Phys. Med. Biol. **44**, 479–493 (1999).
[25] S. Derycke, W. R. De Gersem, B. B. Van Duyse, and W. C. DeNeve, ''Conformal radiotherapy of Stage III nonsmall cell lung cancer: A class solution involving non-coplanar intensity modulated beams,'' Int. J. Radiat. Oncol., Biol., Phys. **41**, 771–777 (1998).
[26] X. H. Wang, R. Mohan, A. Jackson, S. A. Leibel, Z. Fuks, and C. C. Ling, ''Optimization of intensity-modulated 3D conformal treatment plans based on biological indices,'' Radiother. Oncol. **37**, 140–152 (1995).
[27] H. F. Batho, ''Lung corrections in Cobalt-60 beam therapy,'' J. Can. Assoc. Rad. **15**, 79–83 (1964).
[28] S. X. Chang, K. M. Deschesne, T. J. Cullip, S. A. Parker and J. Earnhart, ''A comparison of different intensity modulation treatment techniques for tangential breast irradiation,'' Int. J. Radiat. Oncol., Biol., Phys. **45**, (2000).
[29] E. P. Miller, S. X. Chang, J. Rosenman, and T. Cullip, ''Dose gradient optimization via compensator: Construction and clinical quality assurance,'' Med. Phys. **23**, 1170 (1996).
[30] J. R. Symonds-Tayler and S. Webb, ''Gap-stepped MLC leaves with filler blades can eliminate tongue-and-groove underdoses when delivering IMRT with maximum efficiency,'' Phys. Med. Biol. **43**, 2393–2395 (1998).
[31] R. A. Siochi, ''Minimizing static intensity modulation delivery time using an intensity solid paradigm,'' Int. J. Radiat. Oncol., Biol., Phys. **43**, 671–680 (1999).
[32] E. L. Chaney, T. J. Cullip, and T. A. Gabriel, ''A Monte Carlo study of accelerator head scatter,'' Med. Phys. **21**, 1383–1390 (1994).